Desalination and Water Treatment
www.deswater.com

34(2011)216–221
October

1944-3994/1944-3986
doi: 10/5004/dwt.2011.2864

Preparation and characterization of a new kind of UV-grafted ion-recognition membrane

Lihua Wang[a,*], Chengcheng Tang[a,b], Yanbin Yun[b,*]

[a]*Laboratory of New Materials Institute of Chemistry Chinese Academy of Sciences, Beijing, China*
[b]*College of Environmental Science & Engineering, Beijing Forestry University, Beijing, China*
Tel. +86-132 4173 0890; email: ybyunbj@sohu.com or y.yanbin@unsw.edu.au

Received 3 September 2010; Accepted 3 January 2011

ABSTRACT

A new kind of alkali metal ion-recognized membrane material compound named poly (styrene-co-allyl oxygen)-4-tert butyl-calix [4] arene was synthesized by 4-tert-butyl calyx [4] arene and poly(styrene-co-allyl alcohol) as raw materials. Then a new ion recognition functional membrane was prepared by UV irradiation method via grafting the compound onto the surface of polyacrylonitrile (PAN) micro porous membrane. ATR-FTIR, SEM, AFM and SPM were used to test the surface structure of the functional membrane. The results showed that the functional membrane could form spindle structure on the surface of PAN membrane by the self-assembly way. Control transport experiment for non-functional material (PAA) grafted membrane and functional material grafted membrane were tested in our work, and the data showed that the functional material grafted membrane was able to identify Li^+, Na^+ and K^+ while the PAA grafted membrane have not the ion-recognition ability. The recognition sequence of the functional membrane was K^+>>Na^+>Li^+.

Keywords: UV grafting, Ion-recognition, Calix [4] arene, function membrane, ion transport, PAN membrane

1. Introduction

Ion transport across membranes is one of the most important processes in living cells. Proteins that serve as ion channels or carriers provide this crucial activity. Ion channels have several unusual features, which make them the subject of much biochemical, biophysical, and physiological research. For one, they are highly selective. They discriminate not only between anions and cations, but even between different monovalent and divalent ions, for example, Na^+, K^+, and Ca^+. Other important feature is their efficiency, the energetic barriers in the channel have to be very low, nearly not consume the ATP [1]. Artificial ion channel has been researched for two decades and generally used in metal ion separation, carrier of ion-selective migration and chemical sensor [2–4]. Self-assembly is the most common method to construct ion channel. The influential works included: Percec [5] built columnar cation channel with crown ether by self-assembly, Davis [6–8] used the self-assembly of hydrogen bonding between four guanosine built cation channel, and Sidorov V [9] made a anion channel of Cl^- in the same way.

To simulate the function of ion channel, many chemists or biologists have made their great effort in this field. Therefore, synthetic functional membranes, capable of selectively recognizing and transporting ions or molecules similar to ion channel, represent a challenging target for preparative membrane science. Their potential importance can be imaged by the fact that about 40% of the energy consumption in chemical industry is used for distillation and recrystallization processes. Highly

*Corresponding authors.

Presented at the AMS6/IMSTEC10, The 6th conference of the Aseanian Membrane Society in conjunction with the 7th International Membrane Science and Technology Conference, Sydney Australia, November 22–26, 2010

selective membranes would also simplify numerous separation tasks or detection problems in the fields of biochemical, medical, or even environmental analytical technology [10–12].

Calixarenes represent one of the most important macrocyclic host molecules in supramolecular chemistry, together with crown ether and cyclodextrin in functional membrane research field [13–15]. Because of their basket shape they are suited for the complexation of small molecules and ions. Applications as extractors of metal ions, as carriers in liquid membrane, and as sensors for heavy-metal ions were described [16].

In our course of our studies on the functional ion channel membrane, we became interested in calixarenes because of their basket-shaped structure, which might enable selective transport due to complexation or sieving of distinct ions or molecules. In this paper, amphiphilic copolymer named poly(styene-co-allyl alcohol) and 4-tert-butyl-calix [4] arene were used to prepare of alkali-metal ion-recognized functional membrane material. Then, it was grafted to the surface of PAN membrane using UV irradiation for preparing the ion recognition membrane. The structure and its transport properties of the functional membrane were studied in detail.

2. Experimental

2.1. Material

4-tert-buty-calix [4] arene (98%) was bought from TCI. Poly (styrene-co-allyl alcohol), typical M_n: 1200, typical M_w: 2200, hydroxyl number 255.00 mg KOH/g, was purchased from Sigma Aldrich. 4-(Dimethylamino) ptridine (99%) was obtained from Alfa Aesar. Toluene-4-sulfonyl chloride (98.5%), triethylamine, benzophenone (BP), $NaIO_4$, K_2CO_3, acetone, tetrahydrofuran(THF), 4-(Dimethylamina) chloride and N,N-dimethylfomamide(DMF) were purchased from Sinopharm Chemical Reagent Co.,Ltd. PAN microporous membrane was bought from Shanghai Megavision Membrane Engineering & Technology Co., Ltd.

2.2. Synthesis of poly (styrene-co-allyl oxygen)-4-tert butycalix [4] arene

Firstly, poly (styrene-co-allyl alcohol) and toluene-4-sulfonyl chloride were dissolved in anhydrous THF. Then, triethylamine and 4-(Dimethylamina) chloride were added to the reaction system and mixed by magnetic stirrer. All the processes were carried out in ice bath and the reaction continued for 3–5 h at room temperature under nitrogen protection and magnetic stirrer. Use rapid column chromatography to purify the middle product.

Secondly, the middle product was dissolved in DMF, and then 4-tert-buty calix [4] arene and K_2CO_3 were added. The system reacted 8 h at the temperature of 110°C with magnetic stirring and reflux condensation. After purification, the final product M(d): poly (styrene-co-allyl oxygen)-4-tert buty-calix [4] arene was obtained.

^{1}H NMR(CDCl3, TMS, 400MHz) δ: 0.84876(t, J=16.024, 17H), 1.02048(t, J=7.608, 20H), 1.12974(t, J=10.620, 17H), 1.19427(d, J=6.568, 30H), 2.46092(m, J=9.312,18H), 2.60537(d, J=13.984, 2H), 2.69053(s, 2H), 2.88230(s, 5H), 2.95294(s, 5H), 3.05776(d, J=13.256, 3H), 3.23420(t, J=7.148, 4H), 3.51522(t, J=22.442, 3H), 3.74501(q, J=12.940, 49H), 3.99452(m, J=9.511, 27H), 4.07686(s, 2H), 4.10922(s, 3H), 4.22950(t, J=12.120,24H), 5.29710(s, 1H), 6.45875(d, J=15.348, 3H), 6.65106(d, J=6.620, 2H), 6.83111(q, J=15.224,13H), 6.92977(s, 5H), 7.00196(d, J=6.808, 4H), 7.06427(t, J=3.592, 6H), 7.33365(m, J=8.518, 4H), 7.42645(d, J=7.756, 2H), 7.67357(m, J=10.144, 12H), 7.89706(d, J=8.644, 6H), 8.01742(s, 1H), 8.20500(d, J=8.244, 1H).

2.3. Preparation of UV grafted membrane

Photosensitizer solution (5 wt.%) was prepared by benzophenone, micro scale $NaIO_4$ and acetone solution. Grafting material solution was formed by M(d) and acetone. PAN support membrane was washed by acetone and deionized water for several times. Firstly, immersed the support membrane into photosensitizer solution for 10 min and then dried it in UV grafting reactor under nitrogen atmosphere. Then added grafting material solution into the system, made a sandwich structure by cover it with flat dish. Closed the UV grafting reactor, turned on the 254 nm UV light, irradiated for 30 min with nitrogen protection. After reaction, the grafted membrane was cleaned by acetone and deionized water.

Grafting yield (D) was calculated by: $D=(m_t-m_0)/S$, m_o and m_t was the weight of membrane before and after grafting, S was the area of grafted membrane.

The morphology of membranes was observed by a scanning electron microscope (SEM)(S-3400N), an atomic force microscope (AFM)(Nanoscope III a, Digital Instruments), and scanning probe microscope (SPM) (9600, SHIMADZU).

2.4. Ion transport experiment

The transport properties of the grafted membranes were evaluated using a permeation cell consisting of two square compartments ($V_{half\text{-}cell}$ = 50 ml, membrane area = 0.785 cm^2). Membranes were positioned between the two compartments containing the aqueous phases.

The feed phase was 0.1 mol/l alkali metal chloride solution (NaCl, KCl or LiCl) while the receiving phase was filled with doubly distilled water. Cation permeation was monitored by measuring the conductivity of the receiving phase as a function of time.

Conductivity increment (σ), ion permeation (P) and separation factor (α) were selected as characterizations of the transport experiments.

$$\sigma = \sigma_t - \sigma_o \quad (1)$$

σ_o and σ_t are the conductivity in the beginning and the end of transport experiments.

$$P = \frac{\delta\sigma}{\delta t} \cdot \frac{(V_0 - \Delta V)}{S \cdot \sigma_m \cdot C} \quad (2)$$

$\frac{\delta\sigma}{\delta t}$ is the conductivity growth rate versus time, V_o and ΔV are the solution volume of receiving phase in the beginning and the change in the end of experiment, S is the membrane area, σ_m is the molar conductivity of alkali metal chlorides, C is the concentration of the solution in feed phase.

$$\alpha_{fgm/nfgm} = \frac{P_{fgm}}{P_{nfgm}} \quad (3)$$

P_{fgm} and P_{nfgm} are ion permeations rates of function material grafted membrane and non-function material (PAA) grafted membrane, respectively. $\alpha_{fgm/nfgm}$ is the ion recognition capacity, the larger of $\alpha_{fgm/nfgm}$, and the better of ion recognition capacity.

3. Results and discussion

3.1. UV grafting

Under UV irradiation, BP undergoes a photoreduction by reacting with a hydrogen donor, substrate PAN membranes. The surface free radicals and the semipinacol radicals were generated. The surface free radicals initiate the grafting polymerization of M(d) while the semipinacol radicals initiate homo-polymerization. The grafting dominates the polymerization process owing to the much higher reactivity of surface free radicals. Therefore, the final membranes obtained may be grafted with copolymers in the pores and on the top of the membranes. The grafting yield varied with UV intensity, irradiation time and the composition of the reactant solution. In this paper, we adopted an optimal grafting yield, that is 1.344 mg/cm^2. Fig. 1 was the schematic diagram of UV grafting experiment.

3.2. Chemical and morphological characterization

ATR-FTIR spectra for PAN membrane surface were collected before and after grafting M(d), as shown in Fig. 2. Two typical peaks appeared in each spectrum.

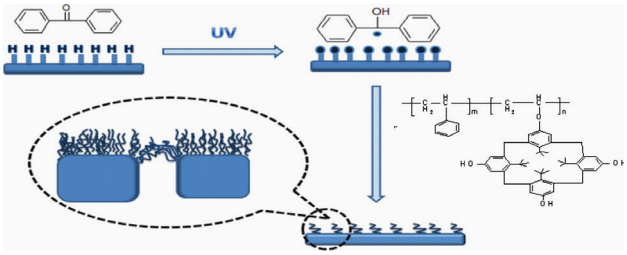

Fig. 1. Schematic diagram of UV grafting experiment.

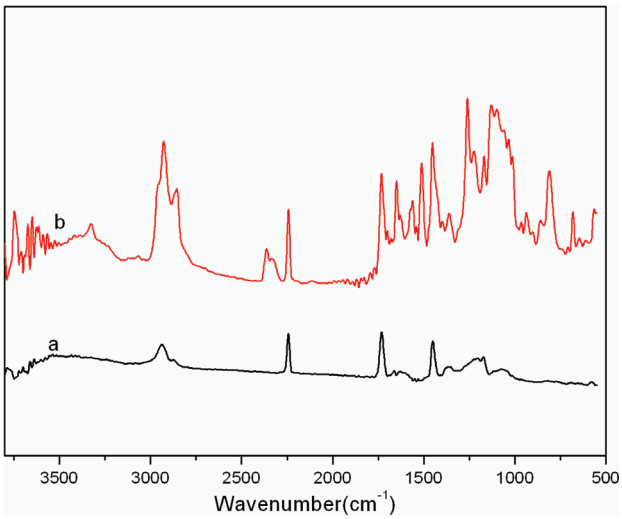

Fig. 2. ATR spectrums of the PAN membrane and the ion recognition membrane (a) PAN nascent membrane (b) ion recognition membrane.

One was at 2242 cm^{-1}, caused by the stretching vibration of cyano groups(-CN), and was the characteristic absorption of PAN. The other one at 1727 cm^{-1} was attributed to the stretching vibration of carbonyl groups. The presence of this absorption in the spectrum of the pure PAN membrane was believed to be caused by the presence of additives. On the other hand, several new absorptions appeared on the line (b). Peak around 3324 cm^{-1} was the stretching vibration of hydroxyl group. Peaks at 2934 and 2858 cm^{-1} could be attributed to the $-CH_3$ and $-CH_2$ absorption. It proved that M(d) which has a lot alcohol hydroxide groups and benzene rings was grafted on the surface of PAN membrane.

Morphology of both the surface and cross-section of nascent and ion recognition membrane was studied by SEM and the images are shown in Fig. 3. From the surface images it can be observed that there were small pores on the surface of the nascent membrane, but these pores disappeared on the surface of ion recognition membrane. From the images of the cross-section that grafting occurred mainly on the surface rather than on the backside. Fig. 4 shows the AFM images

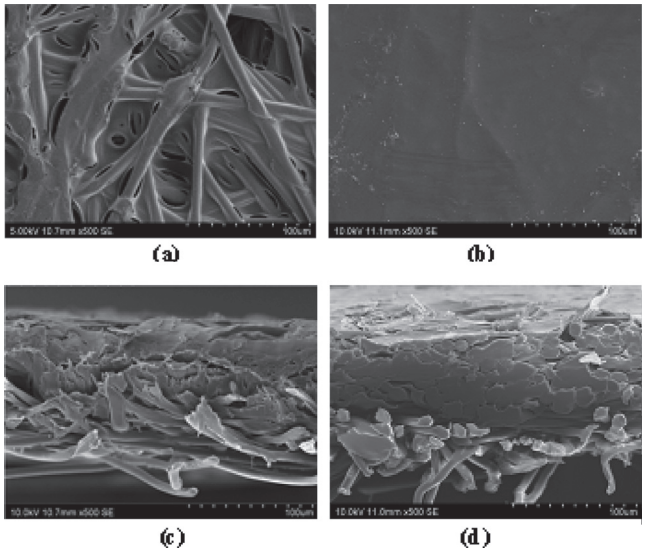

Fig. 3. SEM images of (a) surface of nascent PAN membrane (b) surface of ion recognition (c) cross-side of nascent membrane (d) cross-side of ion recognition membranes.

of the ion recognition membrane. The surface of the ion recognition was dense and the surface roughness increased. Furthermore, the topography of the ion recognition membrane was investigated using SPM. Fig. 5 shows the 2D for 200 nm and 500 nm size scans of the ion recognition membrane. There existed much cone conformation in the SPM images; the average radius of grains is 20–30 nm. These grains closely arranged on the membrane surface, and this may be the results of self-assembly from the M(d).

3.3. Membrane transport experiment

Ion transport across the grafted membrane was studied using a square-shape two-chamber apparatus, as described in the Experimental section. In this process the concentration difference between two chambers is the only driving force. If the membrane was Reverse Osmosis membrane, water molecules would transfer from receiving phase to feed phase and the height of

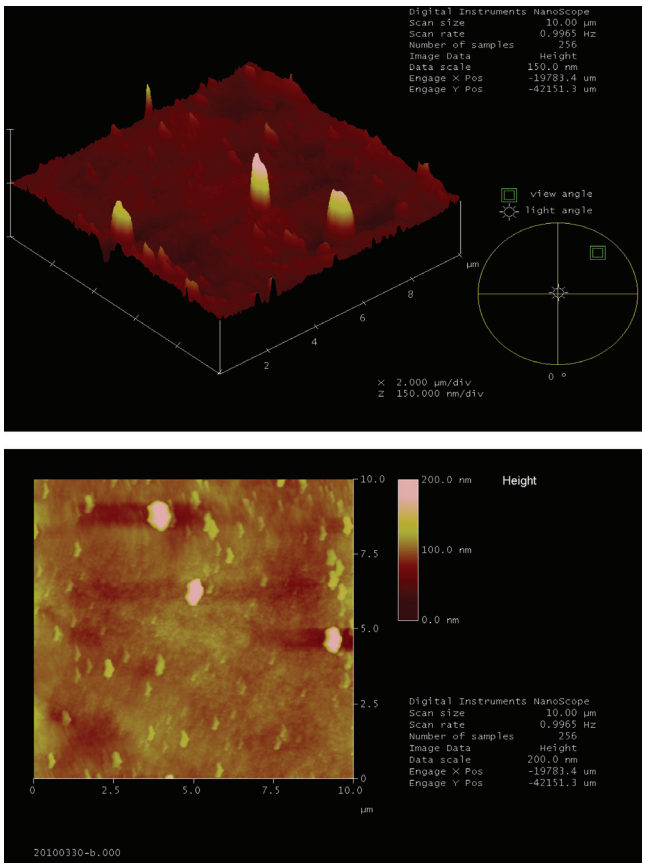

Fig. 4. AFM images of the ion recognition membrane.

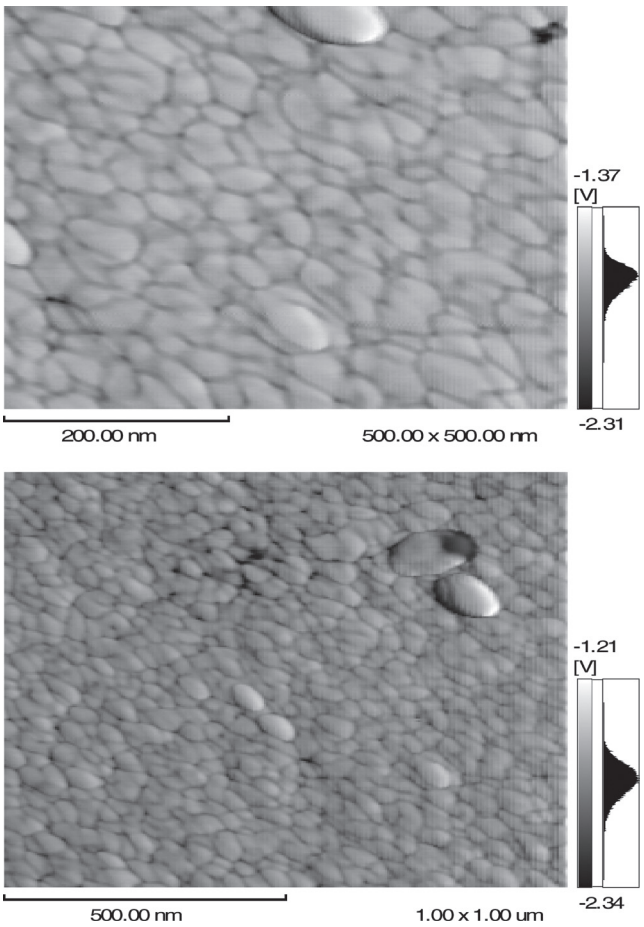

Fig. 5. SPM images of the ion recognition membrane.

the liquid level would change, because of concentration difference. If the membrane is micro-filtration membrane, the water molecules and aquo-metal ions could freely transport, the conductivity would be equal for feed phase and strip phase rapidly. However, for the non-functional grafted membrane and the functional grafted membrane experiments, the height of liquid level were never changed in whole experiment time. And the conductivity of feed phase was higher than that of strip phase too. This phenomenon means that the mechanism of the ion recognition membranes in our work was complex.

The permeation rates of different alkali metal chlorides are plotted in Figs. 6–8 and the corresponding data are as follows. Let us first discuss the permeation rates of NaCl across the ion recognition membrane. As shown in Fig. 6, the Na^+ permeation rate, *P* value, for non-functional grafted membrane and ion recognition membrane were respectively 3.46×10^{-6} cm/s and 40.44×10^{-6} cm/s. The separation factor $\alpha_{fgm/nfgm}$=11.69 >1, which confirmed that ion recognition membrane can recognize Na^+ and allow the ions across the channel formed from the M(d) by self-assembly. And the *P* values are clearly higher than the data reported by Ali Toutianoush [17]. Their results were not more than 12×10^{-6} cm/s for a metal ion channel membranes made from calixarene derivative.

In addition, there was a special phenomenon from the plot of conductivity versus time for NaCl transport experiment. It was clearly that the plot of conductivity versus time could be divided into three stages: slow-grow stage, fast-grow stage and plateau stage. In the first stage, the conductivity enhanced linearly versus time. The reasons were that (1) Na^+ of the feed phase beginning contact with the skin layer of the membrane and then combined with calix [4] arene. The speed of ions transport was low in this stage, $P_{fgm}=12.13\times10^{-6}$ cm/s. In the second stage, When Na^+ sufficiently contacted with the membrane surface, Na^+ began to sharply diffuse in columnar ion channels. In this process, $P_{fgm}=96.24\times10^{-6}$ cm/s, σ increased greatly. In the plateau stage, Na^+ transport was slow again and the $P=34.63\times10^{-6}$ cm/s.

The permeation process for LiCl was shown in Fig. 7. For non-functional grafted membrane (Fig. 7a), the rate of conductivity increase (σ_{nfgm}) and Li^+ permeation (P_{nfgm}) were 6.9 us/cm and 2.81×10^{-6} cm/s respectively. For ion recognition membrane (Fig. 7b), the rate of conductivity increase (σ_{nfgm}) and Li^+ ion permeation (P_{nfgm}) were 14.9 us/cm and 7.14×10^{-6} cm/s. So the separation factor for Li^+ $\alpha_{fgm/nfgm}$=2.54>1, which means the ion recognition membrane has the selectivity for Li^+, but the permeation rate of Li^+ transport was slower. The permeation process for KCl was shown in Fig.8. For K^+ permeation, $P_{nfgm}=1.88\times10^{-6}$ cm/s and $P_{fgm}=197.68\times10^{-6}$ cm/s. The K^+ separation factor $\alpha_{fgm/nfgm}$=105.15 was much larger than 1. It proved that M(d) had a great selectivity for K^+.

The above results mean that the electrostatic (Donnan) rejection of these ions from the equally charged parts of the membrane is only weak and becomes even

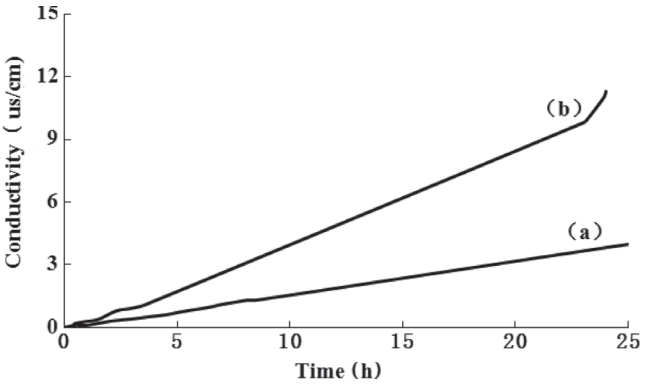

Fig. 7. LiCl transport experiments.

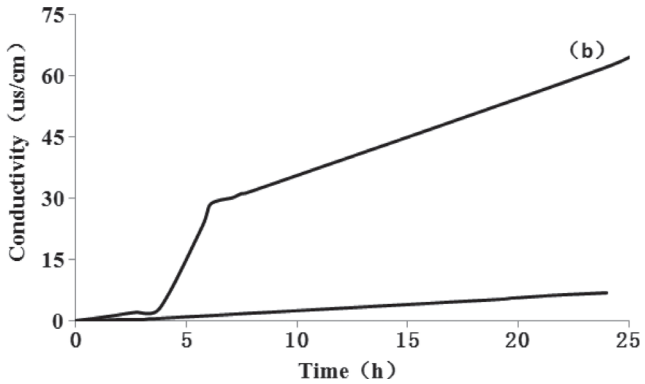

Fig. 6. NaCl transport experiments (a) PAA grafted membrane, (b) ion recognition membrane.

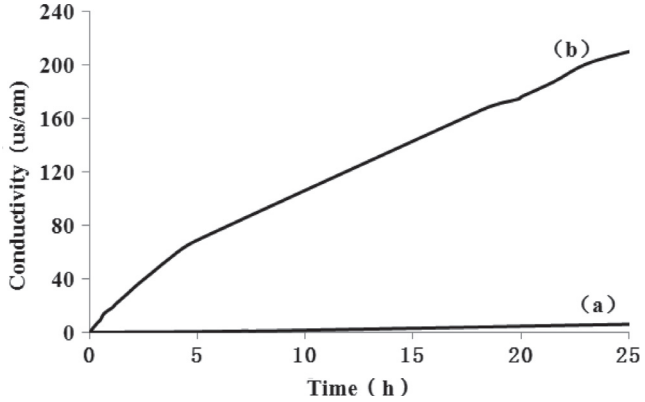

Fig. 8. KCl transport experiments. (a) PAA grafted membrane, (b) ion recognition membrane.

weaker, if the size of the cations increase and the charge density decreases. On the other hand, metal ion formed hydrated ion in aqueous solution. The radius of Li^+ was minimum (68 pm), but the hydrated energy of Li^+ was the maximum, so the action between Li^+ and water molecule was the strongest while K^+ was the weakest. So the self-diffusion coefficients of hydrated ions in water $D_{Li(H2O)n+} < D_{Na(H2O)n+} < D_{K(H2O)n+}$.

In addition, for calyx [4] arene, the cone conformation is most probable. In this conformation, it is especially suitable for binding K^+ rather than Na^+ and Li^+. In further studies, alkali-metal complexation with the calyx [n] arenes will be investigated in more detail.

4. Conclusions

A brand-new kind of alkali metal ion-recognized membrane material named poly (styrene-co-allyl oxygen)-4-tert butyl-calix [4] arene was synthesized by 4-tert-butyl calix [4] arene and poly (styrene-co-allyl alcohol). Then it was grafted on the surface of PAN membrane by UV irradiation, in order to form a functional composite membrane. The function membrane material self-assembled columnar structure with spindle cross-section on the surface of PAN membrane. The recognition sequence of the functional membrane was $K^+>>Na^+>Li^+$ for alkali metal ion.

Acknowledgements

The authors express their thanks to the National Nature Science Foundation of China (No.20704041), National 973 Item (No.2009CB623407), the Fundamental Research Funds for the Central Universities, State Forestry Bureau 948 Project (2009-4-62) and K C. Wong Education Foundation Hong Kong for financial support.

References

[1] F. Hucho and C. Weise, Ligand-Gated ion channels [J], Angew Chem Int Ed Engl., 40 (2001) 3100–3116.
[2] G.W. Gokel and M. Anindita, Synthetic models of cation-conducting channels [J], Chem Sov Rev., 30 (2001) 274–286.
[3] P. Kohli, C.C. Harrell, Z.H. Cao, R. Gasparac, W.H. Tan and C.R. Martin, DNA-functionalized nanochannel membranes with single-base mismatch Selectivity [J], Science, 305 (2004) 984–986.
[4] K.B. Jirage, J. Hulteen and C.R. Martin, Nanotube-based molecular filtration membranes [J], Science, 278 (1997) 655–658.
[5] V. Percec, A.E. Dulcey, V.S.K. Balagurusamy, Y. Miura, J. Smidrkal, M. Peterca, S. Nummelin, U. Edlund, S.D. Hudson, P.A. Heiney, H. Duan, S.N. Magonov and S.A. Vinogradov, Self-assembly of amphiphilic dendritic dipeptides into helical pores [J], Nature, 430 (2004) 764–768.
[6] J.T. Davis and G.P. Spada, Supramolecular architectures generated by self-assembly of guanosine derivatives [J], Chem Sov Rev., 36 (2007) 296–313.
[7] J.T. Davis, G-Quartets 40 Years Later: From 5′-GMP to Molecular Biology and Supramolecular Chemistry [J], Angew Chem Int Ed., 43 (2004) 668–698.
[8] L. Ma, M. Melegari, M. Collombini and J.T. Davis, Large and Stable Transmembrane Pores from Guanosine-Bile Acid Conjugates [J], J. Am. Chem. Soc., 130 (2008) 2938–2939.
[9] V. Sidorov, F.W. Kotch, G. Abdrakhmanova, R. Mizani, J.C. Fettinger and J.T. Davis, Ion channel formation from a calix [4] arene amide that binds HCl [J], J. Am. Chem. Soc., 124 (2002) 2267–2278.
[10] T.M. Fyles, J. Lee, R.D. Rowe and G.D. Robertson, Supramolecular membrane transport: From biomimics to membrane sensors [J], J. Membr. Sci., 321 (2008) 31–36.
[11] Y.F. Zhu, J.L. Shi, W.H. Shen, X.P. Dong, J.W. Feng, M.L. Ruan and Y.S. Li, Stimuli-responsive controlled-release delivery system based on mesoporous silica nanorods capped with magnetic nanoparticles [J], Angew Chem Int. Ed., 44 (2005) 5083–5087.
[12] S. Giri, B.G. Trewyn, M.P. Stellmaker and V.S-Y. Lin, Stimuli-responsive controlled-release delivery system based on mesoporous silica nanorods capped with magnetic nanoparticles [J], Angew Chem. Int. Ed., 44 (2005) 5038–5044.
[13] D.T. Bong, T.D. Clark and M.R.G. Granja, Self-assembling organic nanotubes [J], Angew Chem. Int. Ed. Engl., 40 (2001) 988–1011.
[14] P.K. Eggers, T.M. Fyles, K.D.D. Mitchell and T. Sutherland, Ion channels from linear and branched bola-amphiphiles [J], J. Org. Chem., 68 (2003) 1050–1058 .
[15] N. Madhavan, E.C. Robert and M.S. Gin, A highly active anionselective aminocyclodextrin ion channel [J], Angew Chem. Int. Ed., 44 (2005) 7584–7587.
[16] A. Muhammad, A. Nawash, A. Ibrahim and A. Gülsen, Synthesis and physical studies of polycarbonate of p-tert-butylcalix [4] arene: a highly selective receptor for Na^+ [J], Turk J. Chem., 33 (2009) 647–656.
[17] T. Ali, S. Judit, E.H. Ashraf and T. Bernd, Selective Ion Transport and Complexation in Layer-by-Layer Assemblies of p-Sulfonato-calix [n] arenes and Cationic Polyelectrolytes [J], Adv. Funct. Mater., 15 (2005) 700–708.